Molecular Pharmacology Fast Forward. Published on December 28, 2016 as DOI: 10.1124/mol.116.106963
This article has not been copyedited and formatted. The final version may differ from this version.

Regulator of G-protein Signaling 10 (*Rgs10*) expression is transcriptionally silenced in activated microglia by histone deacetylase activity[i]

Mohammed Alqinyah, Nagini Maganti, Mourad W. Ali, Ruchi Yadav, Mei Gao, Han-Rong Weng, Susanna F. Greer, Shelley B. Hooks

Primary lab of origin: Hooks, UGA

Department of Pharmaceutical and Biomedical Sciences, The University of Georgia, Athens, GA 30602: M.A., M.W.A., H.-R.W., R.Y., M.G., S.B.H

Department of Biology, Georgia State University, Atlanta, GA 30302: N.M., S.F.G.

Molecular Pharmacology Fast Forward. Published on December 28, 2016 as DOI: 10.1124/mol.116.106963
This article has not been copyedited and formatted. The final version may differ from this version.

*Running Title: HDAC-mediated silencing of RGS10 in microglia

To whom correspondence should be addressed:

Shelley B. Hooks,

Department of Pharmaceutical and Biomedical Sciences,

University of Georgia, 250 West Green Street,

Athens, GA, 30602

USA. Tel: 706-542-2189; Fax: (706) 542-5853; E-mail: shooks@uga.edu.

Number of text **pages**: 18

Number of **tables**: 0

Number of **figures**: 7

Number of **references**: 51

Number of words in…

Abstract: 233

Introduction: 602

Discussion: 1488

Abbreviations:

RGS: Regulator of G-Protein Signaling, GPCR: G-protein coupled receptor, GAP: GTPase accelerating protein, TNF-α: tumor necrosis factor α, IL-1β: Interleukin 1-β, TLR: toll-like receptor, LPS: lipopolysaccharide, TSA: trichostatin A, 5-Aza: 5-Aza-2′-deoxycytidine, ChIP: Chromatin immunoprecipitation, pSNL: partial sciatic nerve ligation, DNMT: DNA methyl transferase, HDAC: Histone deacetylase, S1P: Sphingosine 1-phosphate, SAHA: Suberoylanilide hydroxamic acid.

Molecular Pharmacology Fast Forward. Published on December 28, 2016 as DOI: 10.1124/mol.116.106963
This article has not been copyedited and formatted. The final version may differ from this version.

Abstract:

RGS10 has emerged as a key regulator of pro-inflammatory cytokine production in microglia, functioning as an important neuroprotective factor. While RGS10 is normally expressed in microglia at high levels, expression is silenced *in vitro* following activation of TLR4 receptor. Given the ability of RGS10 to regulate inflammatory signaling, dynamic regulation of RGS10 levels in microglia may be an important mechanism to tune inflammatory responses. The goals of the current study were to confirm that RGS10 is suppressed in an *in vivo* inflammatory model of microglial activation and to determine the mechanism for activation-dependent silencing of *Rgs10* expression in microglia. We demonstrate that endogenous RGS10 is present in spinal cord microglia, and RGS10 protein levels are suppressed in the spinal cord in a nerve injury induced neuropathic pain mouse model. We show that the HDAC enzyme inhibitor Trichostatin A blocks the ability of LPS to suppress *Rgs10* transcription in BV-2 and primary microglia, demonstrating that HDAC enzymes are required for LPS silencing of *Rgs10*. Further, we used chromatin immunoprecipitation to demonstrate that H3 histones at the *Rgs10* proximal promoter are deacetylated in BV-2 microglia following LPS activation, and HDAC1 association at the *Rgs10* promoter is enhanced following LPS stimulation. Finally, we have shown that sphingosine 1-phosphate, an endogenous microglial signaling mediator which inhibits HDAC activity, enhances basal *Rgs10* expression in BV-2 microglia, suggesting that *Rgs10* expression is dynamically regulated in microglia in response to multiple signals.

Molecular Pharmacology Fast Forward. Published on December 28, 2016 as DOI: 10.1124/mol.116.106963
This article has not been copyedited and formatted. The final version may differ from this version.

INTRODUCTION

Microglia are central nervous system (CNS)-resident macrophages that serve protective functions to combat infection and clear cellular debris, as well as developmental functions including synaptic pruning (Gehrmann, 1995; Stevens, 2007; Trang, 2011). In addition to these normal physiologic functions, dysregulated microglial activation has been implicated in the initiation and progression of neurodegenerative disorders such as multiple sclerosis, Alzheimer's disease, and Parkinson's disease (Fu, 2014) and in neuropathic pain (Trang, 2011). Identifying signaling pathways regulating microglial functions bears significance in the development of strategies for the treatment of such neurological disorders.

Regulator of G-Protein Signaling 10 (RGS10)[1] has emerged as an important anti-inflammatory regulator in microglia. RGS10 is a member of the RGS superfamily of proteins that deactivate heterotrimeric G-proteins, with profound effects on G-protein coupled receptor (GPCR) signaling in neural diseases (Hurst, 2009; Nishiguchi, 2004; Okahisa, 2011; Vellano, 2011; Zachariou, 2003). RGS proteins are a highly diverse group of proteins that regulate signaling pathways downstream of GPCRs. The classic role of RGS proteins is to regulate the duration and amplitude of G-protein signaling through their ability to function as GTPase activating proteins (GAPs) to accelerate the deactivation of G-proteins by increasing the rate of GTP hydrolysis (Posner, 1999). RGS10 selectively deactivates Gi family G-proteins (Hunt, 1996), and it is expressed at high levels in the brain (Gold, 1997) and immune tissues (Haller, 2002), with specific enrichment in microglia (Waugh, 2005).

Recent studies suggest that RGS10 protein in microglia serves to suppress microglial activation, proliferation, and Nuclear Factor-κB (NF-κB) activity downstream of Toll-like receptor 4 (TLR4) receptors, and loss of RGS10 enhances microglial mediated neuroinflammation and neurotoxicity. RGS10 knock-out mice display significantly more activated microglia in brain tissue (Lee, 2008). Further, in a mouse model of Parkinson's disease, RGS10 knock-out animals display exacerbated dopaminergic neuron cell death compared to wildtype animals. The anti-inflammatory role of microglial RGS10 is also observed and consistently modeled in the mouse microglial cell line BV-2 (Henn, 2009).

Knock-down of RGS10 in BV-2 cells enhances activity of the transcription factor NF-κB and increases expression of inflammatory cytokines including Tumor Necrosis Factor α (TNF-α) and Interleukin 1β (IL-1β) in response to the classic TLR4 activator lipopolysaccharide (LPS) (Henn, 2009). In complementary experiments, RGS10 overexpression suppressed microglial activation, pro-inflammatory cytokine release, and inflammatory neurotoxicity, and inhibited activation of microglial NF-κB (Lee, 2011; Lee, 2008). Therefore, RGS10 is an important regulator of inflammatory signaling in microglia *in vivo* and *in vitro*, and changes in RGS10 levels have significant effects on microglial inflammatory signaling.

RGS10 is normally found in microglia at high levels, but Lee and colleagues have reported that RGS10 protein levels are markedly reduced following microglial activation by LPS or TNFα in microglia (Lee, 2008). Given the ability of RGS10 to regulate inflammatory signaling, understanding the mechanisms that control RGS10 levels in microglia may reveal new therapeutic strategies to address neuroinflammatory disease. The most commonly described mechanism for regulation of RGS protein abundance involves critical post-translational mechanisms that control protein stability (Raveh, 2014; Sjogren, 2012). However, our studies in ovarian cancer cells suggest that *Rgs10* is transcriptionally regulated by DNA and histone targeted epigenetic mechanisms (Ali, 2013a; Cacan, 2014). It is unclear whether and how expression of *Rgs10* in microglia is regulated via epigenetic mechanisms. Further, it is unknown whether *Rgs10* expression can be suppressed by pathological microglial activation and neuroinflammation *in vivo*.

The goals of the current study were to determine if RGS10 is suppressed in an *in vivo* neuroinflammatory model of microglial activation and to determine the mechanism for activation-dependent silencing of *Rgs10* expression in microglia. We observed significant loss of RGS10 in the spinal dorsal horn following nerve injury-induced inflammation, and we define a role for Histone deacetylase (HDAC) regulation of histone acetylation at the *Rgs10* promoter following activation with LPS.

Molecular Pharmacology Fast Forward. Published on December 28, 2016 as DOI: 10.1124/mol.116.106963
This article has not been copyedited and formatted. The final version may differ from this version.

MATERIALS AND METHODS

Cells and Reagents

The murine microglial BV-2 cell line is a well-established model widely used to study microglial functions (Henn et al., 2009) and was a generous gift from Dr. George Hasko at University of Medicine and Dentistry of New Jersey. The BV-2 cell line was generated by infecting primary microglial cell cultures with a v-raf/v-myc oncogene carrying retrovirus (J2) (Blasi et al., 1990). BV-2 cells were maintained in Dulbecco's Modified Eagle's Medium (ATCC) supplemented with 10% FBS (PAA Laboratories, Inc.). Lipopolysaccharide (LPS), H89 dihydrochloride, Trichostatin A (TSA), and 5-Aza-2′-deoxycytidine were obtained from Sigma-Aldrich (St. Louis, MO). Sphingosine 1-phosphate was obtained from Avanti Polar Lipids (Alabaster, Alabama). TNF-α Antagonist III, R-7050 was obtained from Santa Cruz Biotechnology, Inc. (Santa Cruz, CA). For western blot analysis, the following antibodies were used: phospho p44/p42-ERK (Cell Signaling), total ERK(Cell Signaling), anti-RGS10 antibody (C10, Santa Cruz Biotechnology, Inc., Santa Cruz, CA). For ChIP experiments, we used anti-histone H3 and anti-acetylated histone H3 (Millipore, Lake Placid, NY), and anti-HDAC1 (Santa Cruz Biotechnology, Santa Cruz, CA).

Quantitative real-time PCR

mRNA was isolated using Trizol reagent (Invitrogen/Life Technologies, Carlsbad, CA) and cDNA was synthesized from 2 μg of total RNA using the High Capacity Reverse Transcriptase cDNA kit (Applied Biosystems/ Life Technologies). Quantitative real-time polymerase chain reaction was performed using Superscript III kit for RT-PCR (Invitrogen/Life Technologies, Carlsbad, CA) and Power SYBR Green reagent (Applied Biosystems). Reactions were normalized using the housekeeping gene (actin and/or GAPDH, as indicated) and calculations were performed according to the $2^{-\Delta\Delta CT}$ method. Fold change in expression was determined in triplicate in three independent experiments. Primers used were based on algorithm-generated sequences from Primer Bank (http://pga.mgh.harvard.edu/primerbank/). RGS10

Molecular Pharmacology Fast Forward. Published on December 28, 2016 as DOI: 10.1124/mol.116.106963
This article has not been copyedited and formatted. The final version may differ from this version.

Forward: CCT GGA GAA TCT TCT GGA AGA CC, RGS10 Reverse: CTG CTT CCT GTC CTC CGT TTT C, TNFα Forward: CCT GTA GCC CAC GTC GTA G, TNFα Reverse: GGG AGT AGA CAA GGT ACA ACC C, IL1β Forward: GAA ATG CCA CCT TTT GAC AGT G, IL1β Reverse: TGG ATG CTC TCA TCA GGA CAG, Actin Forward: GGC TGT ATT CCC CTC CAT CG, Actin Reverse: CCA GTT GGT AAC AAT GCC ATG T, GAPDH forward: TGG CCT TCC GTG TTC CTA C, GAPDH reverse: GAG TTG CTG TTG AAG TCG CA. All primers were purchased from Integrated DNA Technologies, IDT (Coralville, IA).

Western Blot Analysis

To evaluate protein expression in cell lines, 10^5 cells were lysed in SDS-PAGE sample buffer. The lysates were boiled for five minutes and analyzed using SDS-PAGE. Membranes were incubated with primary antibodies and appropriate HRP-conjugated rabbit secondary antibodies (ThermoScientific, Pierce) and visualized using ECL reagents (ThermoScientific, Pierce). Membranes were subsequently blotted with GAPDH antibodies (Millipore Technologies) as a loading control, and quantified using ImageJ 1.46 software (NIH).

To analyze RGS10 protein expression in the spinal dorsal horn, mice were deeply anesthetized with urethane (1.3–1.5g/kg, i.p.). The L4 to L5 spinal segment was exposed by surgery and removed from the mice, and the animals were then euthanized by cervical dislocation. The dorsal quadrant of the spinal segment ipsilateral to the nerve injury site or sham operation site was isolated. The isolated tissues were quickly frozen in liquid nitrogen and stored at −80 °C for later use. The frozen tissues were homogenized with a hand-held pellet in lysis buffer (50 mM Tris, pH 7.5, 150 mM NaCl, 1 mM EDTA, 0.1% SDS, 1% deoxycholic acid, 2 mM orthovanadate, 100 mM NaF, 1% Triton X-100, 0.5 mM phenylmethylsulfonyl fluoride, 20 μM leupeptin, 100 IU ml^{-1} aprotinin) for 0.5 hr at 37°C. The samples were then centrifuged for 20 min at 12,000 *g* at 4°C and the supernatants containing proteins were collected. The quantification of protein contents was made by the BCA method. Protein samples (40

Molecular Pharmacology Fast Forward. Published on December 28, 2016 as DOI: 10.1124/mol.116.106963
This article has not been copyedited and formatted. The final version may differ from this version.

μg) were electrophoresed in 8 % SDS polyacrylamide gels and transferred to a polyvinylidene difluoride membrane (Millipore, Bedford, MA). The membranes were blocked with 5% milk and incubated overnight at 4°C with antibodies against RGS10 (1:1000, C10, Santa Cruz Biotechnology, Inc., Santa Cruz, CA), or β-actin (1:2000, Sigma-Aldrich, St. Louis, USA) as a loading control. The blots were then incubated for 1 hr at room temperature with the corresponding HRP-conjugated secondary antibody 1:5000; Santa Cruz Biotechnology, CA, USA), visualized in ECL solution (SuperSignal West Pico Chemiluminescent Substrate, Pierce, Rockford, IL, USA) for 1 min, and exposed onto FluorChem HD2 System. The intensity of immunoreactive bands was quantified using ImageJ 1.46 software (NIH). Results were expressed as the ratio of each marker over β-actin control.

Chromatin Immunoprecipitation (ChIP) Assay

ChIP assays were performed as described in Cacan et al., 2014 (Cacan, 2014). Briefly, BV-2 cells were plated at a density of 2.50 x 10^6 in 10 cm-tissue culture plates and the next day the cells were treated with vehicle or LPS (100ng/mL) for 24 hours. Cells were harvested and crosslinked with 1% formaldehyde at room temperature. The crosslinking reaction was stopped by the addition of 0.125 M glycine and cell nuclei were isolated and concentrated by lysing in fresh SDS lysis buffer (1% SDS, 10 mM EDTA, 50 mM Tris pH 8.0, dH_2O) including protease inhibitors followed by flash freezing in liquid nitrogen. Nuclei were sonicated using a Bioruptor water bath sonicator to generate an average of 500-600 bp of sheared DNA. Sonication efficiency was confirmed by subjecting lysates to 1% agarose gel electrophoresis. Sonicated lysates were then precleared with salmon-sperm/agarose beads (Upstate) and 5% of the total lysate was stored as input for normalization. Half of the remaining lysate was immunoprecipitated with 5μg of indicated antibody overnight at 4°C and the other half was immunoprecipitated with control antibody. Following an additional two hour immunoprecipitation with 60μl of salmon-sperm coated agarose beads, all samples were washed with each of the following buffers: low salt buffer (0.1% SDS, 1% Triton X-100, 2 mM EDTA, 20 mM Tris pH 8.0, 150 mM NaCl,

Molecular Pharmacology Fast Forward. Published on December 28, 2016 as DOI: 10.1124/mol.116.106963
This article has not been copyedited and formatted. The final version may differ from this version.

dH_2O), high salt buffer (0.1% SDS, 1% Triton X-100, 2 mM EDTA, 20 mM Tris pH 8.0, 500 mM NaCl, dH_2O), LiCl (0.25 M LiCl, 1% NP40, 1% DOC, 1mM EDTA, 10 mM Tris pH 8.0, dH_2O), and 1xTE. DNA was eluted with SDS elution buffer (1% SDS, 0.1M $NaHCO_3$, dH_2O). Following elution, cross-links were reversed overnight with 5M NaCl at 65°C and immunoprecipitated DNA was isolated using phenol:chloroform:isopropanol mix (Invitrogen/Life Technologies, Carlsbad, CA) as per the manufacturer's instructions. Isolated DNA was quantified by Real time PCR on an ABI prism 7900 (Applied Biosystems, Foster City, CA) using the following primers and probe for RGS10: forward, 5'-ACC CAA GTG TCG TCC AAG TTA-3', reverse, 5'-TGG AGC CTC TGC GGT TTC-3' and probe, 5'-TGC TGG CGC GCT CAG ATC CA -3'; and for GAPDH: forward, 5'- CCA TCC GGG TTC CTA TAA ATA CG -3', reverse, 5'- CGG CCG TCT CTG GAA CA -3' and probe, 5'-CTG CAG CCC TCC CTG GTG CTC TCT-3'. Values generated from Real time PCR reactions were calculated based on standard curves generated, were run in triplicate reactions, and were analyzed using the SDS 2.0 program. RT-PCR experiments were analyzed with both actin and GAPDH internal controls, with similar results.

Mice

C57BL/6J mice were obtained from Harlan laboratories. Male mice of 6–8 week old were used for partial sciatic nerve ligation and sham operation. Primary microglia cultures were prepared from cerebral cortexes of 2 day old neonatal mice pups. Protocols were approved by the Institutional Animal Care and Use Committee at the University of Georgia and were fully compliant with the National Institutes of Health Guidelines for the Use and Care of Laboratory Animals.

Primary microglia isolation

Total glial cultures were isolated from mouse pups at postnatal day 2 (P2) by dissecting total forebrain, removing meninges, dissociating with trypsin, and isolating individual cells by passage over a 40 μm filter. Total cell isolates were plated in T-75 flasks (~three brains per flask), and then the mixed

Molecular Pharmacology Fast Forward. Published on December 28, 2016 as DOI: 10.1124/mol.116.106963
This article has not been copyedited and formatted. The final version may differ from this version.

cultures were grown for 14 days in Eagle's Mimimum Essential Medium (MEM, obtained from ATCC) supplemented with 10% FBS, L-glutamine (glutamax), 4.5 mg/mL glucose, and penicillin/streptomycin. Microglia were isolated by shaking the confluent mixed glial cultures at 250 rpm for 1.5 hours. The supernatant containing microglia was removed, passed through a 35 µm screen, and plated on poly-D-lysine coated 6 well plates (Levison, 1991; Suzumura, 1987).

Immunofluoresence.

Mice were deeply anesthetized with urethane (1.3-1.5 g/kg,i.p.) and transcardially perfused with heparinized phosphate-buffered saline solution (0.1 M PBS) pH = 7.35 followed by a solution of 4% formaldehyde in (0.1 M PBS) pH = 7.35. The L4 and L5 spinal cord was removed and fixed for next 24 hours at 4 °C in fresh 4% formaldehyde. L4- L5 spinal lumbar region was dehydrated with gradient ethanol, and embedded in paraffin. The transverse sections of the spinal cord were sliced at a 10 µm thickness and mounted on microscope slides. After Paraffin-embedded sections were deparaffinized using xylene and ethanol washes, and antigen retrieval treatment was performed by incubating slides in 50 mM sodium citrate (pH8.0) at 80ºC for 30 minutes. Slides were then allowed to cool to room temperature and washed in water and PBS. Tissue was blocked and permeabilized in 0.1X PBS containing 0.1% Triton, 0.5% BSA, and 5% horse serum for 2 hours at room temperature. Primary antibodies (RGS10-1:50; Iba1-1:250) were incubated with the tissue in 0.1X PBS containing 0.5% BSA and 5% horse serum overnight at 4ºC. Following washes in PBS, secondary antibodies (anti-goat 594-fluorophore and anti-rabbit 488-flurophore, both at 1:1000) were incubated with the tissue in PBS for 2 hours at room temperature. Following final washes in PBS, slides were mounted using ProLong Gold with Dapi (ThermoScientific). Slides were imaged using an Olympus U-CMAD3 camera and the Olympus-cell Sens Dimensions software. Exposure and contrast settings were held constant for all images. No manipulation of images was performed, except that the 10X image in figure 2A represents

Molecular Pharmacology Fast Forward. Published on December 28, 2016 as DOI: 10.1124/mol.116.106963
This article has not been copyedited and formatted. The final version may differ from this version.

a composite of two images of the same section (one left, one right) to display the entire dorsal surface of the spinal cord.

pSNL animal model and behavioral tests.

8-week old male wild type C57BL/6J mice were subjected to either pSNL or SHAM surgery groups as described (Seltzer, 1990) Briefly, the left sciatic nerve at the upper thigh was exposed and tightly ligated with 5-0 silk sutures to approximately one-third to one-half its original thickness, and the wound closed with muscle sutures and skin staples. The sham surgery group was subjected to surgical exposure of the sciatic nerve, but without ligation. Behavioral tests were used to determine the development of neuropathic pain in animals with pSNL. Briefly, behavioral tests were conducted in a quiet room with the room temperature at 22°C. To test possible changes in mechanical sensitivity, animals were placed on a wire mesh, loosely restrained under a plexiglass cage (12 × 20 × 15 cm^3) and allowed to acclimate for at least 30 min for rats and 1.5 h for mice. A series of von Frey monofilaments (bending force from 0.07 to 2.00 g) were tested in ascending order to generate response-frequency functions for each animal. Each von Frey filament was applied 5 times to the mid-plantar area of each hind paw from beneath for about 1 s. The response-frequency [(number of withdrawal responses of both hind paws/10) × 100%] for each von Frey filament was determined. Withdrawal response mechanical threshold was defined as the lowest force filament that evoked a 50% or greater response-frequency. This value was later averaged across all animals in each group to yield the group response threshold.

Statistical Analysis

All quantitative data shown are compiled from three independent experimental repeats each performed in duplicate unless otherwise noted. Data were analyzed for statistical differences using an

Molecular Pharmacology Fast Forward. Published on December 28, 2016 as DOI: 10.1124/mol.116.106963
This article has not been copyedited and formatted. The final version may differ from this version.

analysis of variance (ANOVA) followed by Bonferroni's Multiple Comparison test or Tukey's test between groups. *p < 0.05 **p < 0.01 and ***p < 0.001 indicate the levels of significance.

RESULTS

Suppression of RGS10 expression enhances GPCR signaling in BV-2 microglia

Previous studies have demonstrated the effect of RGS10 suppression on multiple inflammatory signaling pathways in microglia. To demonstrate the effect of RGS10 suppression on a classic GPCR signaling pathway, we treated BV-2 microglial cells with control or RGS10-targeted siRNA, and determined the effect of CXCL12/Sdf-1 stimulated ERK Map kinase phosphorylation. Knock-down of RGS10 by 70% had no effect on basal MAP kinase phosphorylation, but significantly (p=0.045) increased CXCL12 stimulated MAP kinase phosphorylation (Figure 1). This suggests that endogenous mechanisms that control the level of RGS10 expression may significantly impact the strength of GPCR signaling pathways.

LPS silencing of RGS10 transcript and protein expression in BV-2 microglia

RGS10 protein levels are reportedly suppressed in microglia following activation by LPS or TNF-α, but early studies suggested that the effect may not follow a typical dose-response (Lee, 2008), and the effect on transcription of *Rgs10* was not defined. To further characterize RGS10 suppression, we analyzed *Rgs10* transcript and RGS10 protein levels after treating mouse microglial BV-2 cells with increasing doses of LPS using qRT-PCR and western blotting, respectively. LPS treatment resulted in suppression of both *Rgs10* transcript (measured at 4 hours, Figure 2A) and RGS10 protein (measured at 24 hours, Figure 2B) in a dose-dependent fashion, with maximal effects observed at 1 μg/mL. We simultaneously measured LPS induced TNFα inflammatory cytokine transcript production to confirm robust microglial activation (Figure 2A, lower panel). The fold change and dose dependency of

Molecular Pharmacology Fast Forward. Published on December 28, 2016 as DOI: 10.1124/mol.116.106963
This article has not been copyedited and formatted. The final version may differ from this version.

suppression of *Rgs10* transcript expression was very similar to protein expression changes, suggesting a primarily transcriptional mechanism of silencing. A time course of LPS treatment (100 ng/mL) showed *Rgs10* transcript was maximally inhibited at approximately 6 hours and remained suppressed up to 72 hours (Figure 2C). These results demonstrate activation of microglia by LPS triggers transcriptional suppression of *Rgs10* while enhancing pro-inflammatory cytokine expression.

Silencing of endogenous RGS10 in an in vivo inflammatory model of microglial activation

Microglial activation and, specifically, endogenous activation of microglial TLR4 receptors are directly implicated in the development of pain sensitization in the mouse partial sciatic nerve ligation (pSNL) model of neuropathic pain (Bettoni, 2008; Raghavendra, 2003). This suggests that the TLR4 mediated suppression of RGS10 we have observed *in vitro* may occur endogenously in the spinal cord following pSNL injury. To test this prediction, we first confirmed RGS10 levels in resident microglia of the spinal dorsal horn. Immunofluoresence staining with RGS10 and Iba1 microglial marker show robust RGS10 abundance in the spinal cord, and clear co-localization in Iba-1 positive cells with distinct microglial morphology (Figure 3A). We next performed SHAM or pSNL surgeries on three mice each, and assessed RGS10 protein levels in the spinal dorsal horn three days post surgery, at which time robust microglial activation occurs (Weng, 2014). Baseline pain sensitivity was determined immediately prior to surgeries, and again three days after surgery immediately before sacrifice to confirm the development of pain sensitization in the pSNL animals (data not shown). The L4-L5 region of the spinal cord was isolated and total lysates were subjected to western blotting with RGS10 and β-actin control antibodies. Our results show an approximately 50% reduction in total RGS10 level in the spinal cord of pSNL animals, suggesting that RGS10 silencing occurs *in vivo* under conditions that trigger endogenous microglial activation (Fig. 3B).

The role of DNMT and HDAC enzymes in LPS-mediated RGS10 silencing in microglia

Molecular Pharmacology Fast Forward. Published on December 28, 2016 as DOI: 10.1124/mol.116.106963
This article has not been copyedited and formatted. The final version may differ from this version.

We previously reported that the *Rgs10* gene is epigenetically suppressed in chemoresistant ovarian cancer cells via both DNA Methyl Transferase (DNMT) and Histone Deacetylase (HDAC) activities (Hooks, 2010). However, the development of chemoresistance and the accompanying suppression of RGS10 reflects chronic culturing conditions that cause global gene expression changes, and it is therefore unclear whether the acute silencing of *Rgs10* observed in microglia in response to LPS may involve distinct mechanisms. To test whether *Rgs10* expression is regulated by DNMT enzymes in BV-2 cells following acute LPS treatment, we analyzed *Rgs10* transcript and RGS10 protein expression following pharmacological inhibition of DNMT enzymes. BV-2 cells were treated with vehicle or LPS (10 ng/mL) with or without co-treatment with 5-Aza (10 μM). In experiments measuring transcript, cells were treated with LPS for six hours; in experiments measuring protein expression, cells were treated with LPS for 48 hours. In both experiments, either 5-Aza or vehicle control was added to cells 1 hour before LPS and then maintained in media during the LPS treatment. Under these conditions, 5-Aza treatment did not alter basal or LPS-treated *Rgs10* transcript or RGS10 protein expression levels (Figure 4A, B), suggesting that DNMT enzymes do not play a major role in regulating *Rgs10* expression in BV-2 microglia under these conditions.

To test whether *Rgs10* expression is regulated by HDAC enzymes in BV-2 cells, we analyzed *Rgs10* transcript expression following pharmacological inhibition of HDAC enzymes using the HDAC inhibitor, trichostatin A (TSA). Basal *Rgs10* transcript expression was increased in BV-2 cells in a dose dependent fashion following 24 hour TSA treatment with maximal effect observed at 250 nM, suggesting that basal *Rgs10* gene expression is epigenetically regulated through HDAC activity (Fig. 5A). Next, we tested whether TSA could block LPS-induced *Rgs10* suppression in BV-2 cells. To that end, we treated BV-2 cells with vehicle or LPS (10 ng/mL) for six hours following pre-treatment with TSA (100 nM) for one hour. TSA was also maintained in the cell media during the LPS treatment. We found that one hour pre-treatment increased basal activity and significantly blocked LPS-stimulated suppression of *Rgs10* transcript expression. To explore the ability of TSA to block the effect of higher

Molecular Pharmacology Fast Forward. Published on December 28, 2016 as DOI: 10.1124/mol.116.106963
This article has not been copyedited and formatted. The final version may differ from this version.

doses of LPS, we determined that a 20 hour pre-treatment with 250 nM TSA fully blocked the effect of 1 μg/mL LPS on *Rgs10* expression (Fig. 5C). Finally, we also confirmed that the effect of TSA on *Rgs10* expression was not limited to transcript but resulted in restored RGS10 protein levels, as shown in Figure 5E. These results suggest that LPS-induced *Rgs10* suppression in BV-2 cells is epigenetically mediated via histone acetylation of the RGS10 promoter.

BV-2 cells were selected as a model system to study the mechanism of silencing because they recapitulate RGS10 silencing and they are a widely used reliable model of microglial signaling (Henn, 2009). However, it is possible that gene regulation in an immortalized cell culture model does not accurately represent regulation in primary microglia. To address this concern, we isolated primary microglia from neonatal mice brain tissue to assess regulation of *Rgs10* expression by LPS and TSA. Using immunostaining with Iba1 (microglia), GFAP (astrocytes), and NeuN (neurons), we confirmed our microglia-enriched cultures contain approximately 90-95% microglia, with a few astrocytes and no neurons detectable (data not shown). In these primary cultures, one hour pre-treatment with 100 nM TSA fully blocked silencing of *Rgs10* expression stimulated by LPS (10 ng/mL, 6 hours), consistent with the effects observed in BV-2 cells (Fig. 5D).

Role of TNFα in LPS-stimulated RGS10 silencing

We also quantified *TNFα* transcript expression following LPS and/or TSA treatment using qRT-PCR, and found that the trend in *TNFα* transcript expression was opposite that of RGS10 expression; LPS significantly enhanced *TNFα* expression and HDAC inhibition blocked LPS-induced *TNFα* production (Figure 6A). Previous studies by Lee et al. show that TNFα as well as LPS can trigger suppression of RGS10 expression in microglia (Lee, 2008), suggesting that LPS-mediated suppression of *Rgs10* may, in part, be secondary to LPS-stimulated *Tnfα* production and TNFα-mediated suppression of RGS10. Further, given that HDAC inhibition by TSA suppressed *Tnfα* as well as enhanced *Rgs10* expression, it is possible that the effect of TSA on *Rgs10* expression could also be

Molecular Pharmacology Fast Forward. Published on December 28, 2016 as DOI: 10.1124/mol.116.106963
This article has not been copyedited and formatted. The final version may differ from this version.

secondary to effects on *Tnfα* expression. To clarify the role of TNFα in LPS-mediated suppression of *Rgs10*, we determined the effect of inhibition of TNFα receptor activation on LPS-stimulated *Rgs10* suppression. Cells were treated with LPS as above with or without a one hour pre-treatment with 10 μM R-7050, a TNFα receptor inhibitor, and *Rgs10* transcript was quantified as above. TNFα receptor inhibition had no effect on LPS stimulated *Rgs10* transcript or protein suppression, indicating that TNFα receptor activity is not required for LPS effects on *Rgs10* (Fig. 6B, D). The same treatment with R-7050 had a significant effect on LPS-stimulated IL-1β production, confirming that the compound is active in the conditions tested (Fig. 6C).

LPS effects on histone acetylation and HDAC1 recruitment at the RGS10 promoter in microglia

The ability of TSA to enhance *Rgs10* expression and block LPS-mediated silencing suggests a role for HDAC enzymes in controlling *Rgs10* expression, but TSA is not completely selective for HDAC enzymes and may have off-target effects. To directly test the role of histone acetylation in the regulation of *Rgs10* expression in BV-2 cells, we performed chromatin immunoprecipitation (ChIP) assays to quantify the amount of acetylated histones and HDAC1 enzyme bound to the proximal *Rgs10-1* promoter with and without LPS treatment (100 ng/ml, 24 hours). LPS treatment resulted in a nearly 5-fold increase in the association of HDAC1 at the *Rgs10-1* promoter (Figure 7A). The change in HDAC1 binding was accompanied by a marked decrease in acetylated histone H3 levels at the RGS10 promoter, while total histone H3 levels remained similar (Figure 7B, C). These results suggest the *Rgs10* gene is epigenetically silenced in microglia following LPS stimulation via HDAC1 recruitment and decreased histone H3 acetylation at the *Rgs10-1* promoter.

Molecular Pharmacology Fast Forward. Published on December 28, 2016 as DOI: 10.1124/mol.116.106963
This article has not been copyedited and formatted. The final version may differ from this version.

Sphingosine 1-phosphate enhances RGS10 expression and alters histone acetylation at *Rgs10* promoter.

Our results suggest that activation of TLR4 receptors by LPS triggers a signaling cascade that culminates in recruitment of HDAC to *Rgs10* promoters, resulting in transcriptional silencing. However, the ability of TSA to dramatically enhance basal *Rgs10* expression (Fig. 5A) suggests that even in the absence of an activation signal, HDAC activity suppresses *Rgs10* expression. This suggests that signaling pathways that inhibit HDAC activity in microglia may increase RGS10 expression in resting microglia. Sphingosine 1-phosphate (S1P) in an endogenous bioactive lipid mediator in neurons and glia, and S1P activates G-protein coupled receptors in microglia to regulate inflammatory signaling (Durafourt, 2011; Kimura, 2007; Nayak, 2010; Noda, 2013). S1P has also been shown to inhibit HDAC1 enzymes via receptor-independent nuclear mechanisms (Hait, 2009). Therefore, we tested the effect of S1P on *Rgs10* expression and histone modifications at the *Rgs10* promoter. BV-2 cells treated with S1P showed a five-fold increase in *Rgs10* transcript expression following 48 hours of S1P treatment (Figure 8A). To confirm that the ability of S1P to regulate *Rgs10* expression reflected a change in HDAC activity, we determined histone acetylation levels at the proximal *Rgs10-1* promoter following S1P treatment, and observed a significant increase in H3 histone acetylation, with no change in total H3 histone levels (Fig. 8B). Together, our data demonstrate that histone acetylation of the *Rgs10* promotor is dynamically regulated in microglia by endogenous signals to increase or decrease expression of this critical regulator of inflammatory signaling.

Molecular Pharmacology Fast Forward. Published on December 28, 2016 as DOI: 10.1124/mol.116.106963
This article has not been copyedited and formatted. The final version may differ from this version.

DISCUSSION

Microglia, CNS resident macrophages, have been implicated in the initiation and progression of multiple neurological disorders including neurodegenerative disease and neuropathic pain (Schwartz, 2013). Microglia are activated by inflammatory agents such as LPS, resulting in activation of NF-κB transcriptional pathways and production of pro-inflammatory cytokines. RGS10 has emerged as an important regulator of pro-inflammatory cytokine production in microglia. Microglia from RGS10 knock-out mice show enhanced NF-κB reporter activity and higher expression of inflammatory cytokines including TNF-α and IL-1β following LPS stimulation, and restoration of RGS10 normalizes responses to LPS (Lee, 2011; Lee, 2008). Further, RGS10 loss enhances LPS-induced dopaminergic neuronal death (Lee, 2008), while restoration of RGS10 rescues these neurons (Lee, 2011). Importantly, siRNA-mediated reduction of microglial RGS10 expression by 50-75% was sufficient to significantly enhance cytokine levels (Lee, 2008). Our data also show that suppression of RGS10 by 70% significantly enhances chemokine signaling, demonstrating that even partial loss of RGS10 has an important impact on inflammatory signaling in microglia. While RGS10 is normally present in microglia at high levels, expression is silenced by activation of TLR4 or TNFα receptors. Following activation by the TLR4 activator LPS, microglial *Rgs10* transcript expression levels were reduced by up to 75%, comparable to the fold suppression sufficient to amplify NF-κB signaling and inflammatory cytokine production (Lee, 2008). This suggests that silencing of RGS10 is sufficient to amplify microglial inflammatory signaling in a feed-forward mechanism that may contribute to the dysregulation of inflammatory signaling in chronic neuroinflammation and disease. Understanding the molecular mechanisms of RGS10 suppression in microglia may reveal novel targets for therapeutic intervention in diseases with underlying chronic neuroinflammation. With this in mind, we sought to define the molecular mechanism of RGS10 suppression following TLR4 activation *in vitro*.

In this study we find that activation of microglia by LPS triggers a rapid and robust transcriptional silencing of *Rgs10*. Lee et. al previously reported that a low dose of LPS (10 ng/ml)

Molecular Pharmacology Fast Forward. Published on December 28, 2016 as DOI: 10.1124/mol.116.106963
This article has not been copyedited and formatted. The final version may differ from this version.

decreased RGS10 protein in BV-2 cells, while a higher dose of LPS (1 μg/ml) did not change RGS10 protein level (Lee, 2008). Here we report that *Rgs10* transcript and protein levels were suppressed in BV-2 cells in a typical dose-dependent fashion. LPS-induced suppression of *Rgs10* transcript reflected and preceded the reduction in protein levels, which suggests that the reduction in RGS10 protein level observed following LPS treatment is mainly due to inhibition of transcription.

Previously, we reported an epigenetic regulation of *Rgs10* expression in chemoresistant ovarian cancer cells mediated by the combined activities of HDAC and DNMT enzymes. Here, we investigated whether *Rgs10* expression in microglia is regulated in a similar mechanism after acute LPS treatment. We found that the HDAC inhibitor TSA significantly enhances basal *Rgs10* transcript expression and blocks LPS-induced *Rgs10* suppression in microglia, while the DNMT inhibitor had no effect under the conditions tested. We further show that LPS increases HDAC1 association and decreases histone H3 acetylation at the *Rgs10* promoter, observations which strengthen the notion that *Rgs10* genes are epigenetically silenced via histone deacetylation in LPS-activated microglia. We also show that HDAC inhibition caused a decrease in LPS-mediated pro-inflammatory cytokine TNFα (and IL-1β, not shown) production in microglia. Consistent with our observations, HDAC inhibitors have been reported to possess anti-inflammatory effects by lowering pro-inflammatory cytokine production in microglia (Suh, 2010). The HDAC inhibitor SAHA has been shown to reduce the production of pro-inflammatory cytokines production in activated microglia (Faraco, 2009), while TSA reduces pro-inflammatory cytokine production in microglia and reduces brain injury in a model of LPS-sensitized neonatal hypoxic-ischemia (Fleiss, 2012).

The mouse *Rgs10* gene contains two transcriptional start sites, yielding two transcript isoforms with distinct first exons, and four common exons (Haller, 2002; Lee, 2015). Mouse transcripts *mRgs10-1* and *mRgs10-2* correspond to human transcripts with conserved exon structure and encoding highly conserved human RGS10 protein isoforms RGS10a (181aa) and RGS10b (167 aa). A third human transcript (173aa) has been proposed, resulting from an alternate transcriptional start site upstream of

Molecular Pharmacology Fast Forward. Published on December 28, 2016 as DOI: 10.1124/mol.116.106963
This article has not been copyedited and formatted. The final version may differ from this version.

the first shared exon (Hunt, 1996), but the relevance of this transcript in mouse cells is unclear (Haller, 2002). We have shown that *Rgs10-1* is the predominant form expressed in human cancer cells, *Rgs10-1* is selectively silenced in chemoresistant cells, and that HDAC1 is recruited to the unique *Rgs10-1* promoter in these cells (Ali, 2013a; Ali, 2013b; Cacan, 2014; Hooks, 2010). Our studies and others have indicated that the long isoform (*Rgs10-1* → RGS10a) is also the predominantly expressed form in microglia and other immune cells (Lee, 2015). For these reasons, our studies in microglia focused on regulation of the mouse *Rgs10-1* transcript, and ChIP experiments were targeted to the mouse *Rgs10-1* proximal promoter.

Microglial activation in the spinal dorsal horn enhances nociception and is a causative factor in central sensitization that contributes to neuropathic pain (Raghavendra, 2003; Zhuo, 2011). The pSNL model of injury-induced neuropathic pain results in robust microglial activation and spinal sensitization. During nerve injury-induced sensitization, endogenous mediators activate microglial TLR4 receptors, which trigger production of pro-inflammatory cytokines (Bettoni, 2008; Tanga, 2005; Wu, 2010). Blocking either microglial activation or endogenous TLR4 receptors has been shown to attenuate neuropathic pain (Raghavendra, 2003; Saito, 2010; Sorge, 2011; Yoon, 2012). Further, enhanced HDAC activity is observed in the spinal cord following nerve injury (Lu, 2013; Lv, 2011), and HDAC inhibitors reduce inflammatory cytokine release and neuroinflammation (Blanchard, 2005; Lv, 2011). Thus, the pSNL model of neuropathic pain is suitable for the in vivo study of molecular signaling pathways in microglia activated by TLR4.

We have demonstrated that RGS10 is abundant in the spinal cord, with confirmed localization in microglia. Non-microglial cell-types also stain positively for RGS10, consistent with reports of predominantly microglial and lesser neuronal expression in brain (Waugh, 2005). Following pSNL injury, we observe down-regulation of RGS10 protein expression by about 50% in spinal dorsal horn as measured by western blotting in total L4-L5 spinal dorsal horn tissue. Our observation that RGS10 is suppressed in the spinal cord in the pSNL model provides supporting evidence that the suppression

observed in cultured BV-2 and primary microglia also occurs *in vivo*. However, our approach likely underestimates the cellular suppression of RGS10; given that RGS10 is predominantly expressed in microglia, the expansion of microglia during inflammation following pSNL likely masks the degree of RGS10 suppression in individual microglial cells. Further, the expression of RGS10 in neurons, although less than microglia, also limits quantitative interpretation of the degree of suppression in microglia. Thus, future studies should evaluate RGS10 levels in individual microglia isolated from *in vivo* neuroinflammation models. It will also be important for future studies to determine if HDAC inhibitors, which are known to inhibit inflammatory signaling, also restore *Rgs10* expression in the spinal cord, and if this effect contributes to their ability to impact inflammation. Tansey and colleagues have shown that re-introduction of RGS10 protein expression in microglia from knock-out animals normalizes inflammatory signaling and dopaminergic neuron cell death *in vivo (Lee, 2011)*. Therefore, strategies that restore RGS10 levels in microglia may blunt neuroinflammation and associated diseases.

In recent years RGS proteins have emerged as promising novel drug targets in diverse disease states, but progress has lagged due to the lack of traditional small molecule ligand or substrate interaction sites. Strategies to target regulation of RGS protein expression have focused on post-translational mechanisms that control protein stability (Raveh, 2014; Sjogren, 2012). In contrast, our data suggest predominantly transcriptional regulation of *Rgs10* expression. Our results demonstrate that *Rgs10* silencing is completely reversible with small molecule HDAC inhibitors and provide proof of concept for targeting RGS10 suppression in neuroinflammatory disease models. Multiple HDAC inhibitors are being assessed in clinical trials, but specificity, pharmacokinetic features and toxicity remain significant barriers to the use of broad spectrum HDAC inhibitors in CNS diseases. Thus, more selective pharmacological approaches are needed to target *Rgs10* silencing.

A potential alternative to targeting HDAC enzymes directly in order to regulate *Rgs10* expression is to target more selective pathways that may indirectly modulate HDAC activity. S1P

Molecular Pharmacology Fast Forward. Published on December 28, 2016 as DOI: 10.1124/mol.116.106963
This article has not been copyedited and formatted. The final version may differ from this version.

activates a family of GPCRs, including several expressed in microglial cells, and S1P is a key regulator of microglial activity (Blaho, 2014; Nayak, 2010; Noda, 2013; Tham, 2003). Our results here show that S1P may enhance *Rgs10* expression through regulation of HDAC. Notably, the time course of S1P effects on RGS10 expression (48 hours) was much longer than that of LPS effects on *Rgs10* expression (6 hours), and it remains to be determined if S1P receptor activation is sufficient to reverse LPS mediated silencing of RGS10. However, the involvement of GPCRs in regulating *Rgs10* expression offers another opportunity for therapeutic intervention, as GPCRs are relatively easy to target with reasonable selectivity compared to HDACs. Strikingly, the S1P receptor functional antagonist FTY-720 (Fingolimod, Gilenya) has been approved for use in relapsing-remitting multiple sclerosis (MS), and a recent study demonstrated that RGS10 knock-out animals exhibit blunted symptoms in the EAE model of MS (Lee, 2016). Given the role of microglial activation in MS pathology, it is tempting to postulate a connection between our observations connecting S1P receptors and RGS10 in microglia with these findings in models of MS. However, the predicted mechanisms of action of both FTY-720 and RGS10 in MS models are based on their effects on peripheral immune cells, not microglia, so the relevance of the observed regulation in microglia to MS is unclear at this time.

Summary

In this study, we demonstrate dose-dependent suppression of *Rgs10* in response to LPS activation in microglia, demonstrate that the HDAC inhibitor TSA blocks the ability of LPS to suppress *Rgs10* expression, and demonstrate HDAC1 recruitment and H3 histones deacetylation at the *Rgs10-1* proximal promoter following LPS stimulation. These observations suggest that LPS-stimulated silencing of *Rgs10* expression is rapid, robust, and reversible in BV-2 microglial cells, and this model system reflects the mechanism observed in primary microglia. We further show that activation of microglial S1P receptors increases *Rgs10* expression, demonstrating that *Rgs10* expression may be precisely dialed up or down in microglia in response to multiple cues. Finally, we demonstrate that RGS10 is suppressed in an *in vivo* mouse model of injury-induced inflammation. Together, our results suggest

Molecular Pharmacology Fast Forward. Published on December 28, 2016 as DOI: 10.1124/mol.116.106963
This article has not been copyedited and formatted. The final version may differ from this version.

that the ability of RGS10 to regulate microglial inflammatory pathways can be modulated by various pathways through HDAC regulation of *Rgs10* expression with significant implications on neuroinflammatory disease states.

Authorship Contributions:

Participated in research Design: M.A., N.M., H-R.W., S.F.G., S.B.H.

Conducted experiments: M.A., N.M., M.W.A., R.Y., M.G.

Performed data analysis: M.A., N.M., S.F.G., S.B.H

Wrote or contributed to writing of the manuscript: M.A., S.B.H.

Molecular Pharmacology Fast Forward. Published on December 28, 2016 as DOI: 10.1124/mol.116.106963
This article has not been copyedited and formatted. The final version may differ from this version.

References

Ali MW, Cacan E, Liu Y, Pierce JY, Creasman WT, Murph MM, Govindarajan R, Eblen ST, Greer SF and Hooks SB (2013a) Transcriptional suppression, DNA methylation, and histone deacetylation of the regulator of G-protein signaling 10 (RGS10) gene in ovarian cancer cells. *PloS one* **8**(3):e60185.

Ali MW, Cacan E, Liu Y, Pierce JY, Creasman WT, Murph MM, Govindarajan R, Eblen ST, Greer SF and Hooks SB (2013b) Transcriptional suppression, DNA methylation, and histone deacetylation of the Regulator of Gprotein Signaling 10 (RGS10) gene in ovarian cancer cells. *PLOS ONE* **in press**.

Bettoni I, Comelli F, Rossini C, Granucci F, Giagnoni G, Peri F and Costa B (2008) Glial TLR4 receptor as new target to treat neuropathic pain: efficacy of a new receptor antagonist in a model of peripheral nerve injury in mice. *Glia* **56**(12):1312-1319.

Blaho VA and Hla T (2014) An update on the biology of sphingosine 1-phosphate receptors. *Journal of lipid research*.

Blanchard F and Chipoy C (2005) Histone deacetylase inhibitors: new drugs for the treatment of inflammatory diseases? *Drug discovery today* **10**(3):197-204.

Cacan E, Ali MW, Boyd NH, Hooks SB and Greer SF (2014) Inhibition of HDAC1 and DNMT1 modulate RGS10 expression and decrease ovarian cancer chemoresistance. *PloS one* **9**(1):e87455.

Durafourt BA, Lambert C, Johnson TA, Blain M, Bar-Or A and Antel JP (2011) Differential responses of human microglia and blood-derived myeloid cells to FTY720. *Journal of neuroimmunology* **230**(1-2):10-16.

Faraco G, Pittelli M, Cavone L, Fossati S, Porcu M, Mascagni P, Fossati G, Moroni F and Chiarugi A (2009) Histone deacetylase (HDAC) inhibitors reduce the glial inflammatory response in vitro and in vivo. *Neurobiology of disease* **36**(2):269-279.

Fleiss B, Nilsson MK, Blomgren K and Mallard C (2012) Neuroprotection by the histone deacetylase inhibitor trichostatin A in a model of lipopolysaccharide-sensitised neonatal hypoxic-ischaemic brain injury. *Journal of neuroinflammation* **9**:70.

Fu R, Shen Q, Xu P, Luo JJ and Tang Y (2014) Phagocytosis of Microglia in the Central Nervous System Diseases. *Molecular neurobiology*.

Gehrmann J, Matsumoto Y and Kreutzberg GW (1995) Microglia: intrinsic immuneffector cell of the brain. *Brain research Brain research reviews* **20**(3):269-287.

Gold SJ, Ni YG, Dohlman HG and Nestler EJ (1997) Regulators of G-protein signaling (RGS) proteins: region-specific expression of nine subtypes in rat brain. *The Journal of neuroscience : the official journal of the Society for Neuroscience* **17**(20):8024-8037.

Hait NC, Allegood J, Maceyka M, Strub GM, Harikumar KB, Singh SK, Luo C, Marmorstein R, Kordula T, Milstien S and Spiegel S (2009) Regulation of histone acetylation in the nucleus by sphingosine-1-phosphate. *Science* **325**(5945):1254-1257.

Haller C, Fillatreau S, Hoffmann R and Agenes F (2002) Structure, chromosomal localization and expression of the mouse regulator of G-protein signaling10 gene (mRGS10). *Gene* **297**(1-2):39-49.

Henn A, Lund S, Hedtjarn M, Schrattenholz A, Porzgen P and Leist M (2009) The suitability of BV2 cells as alternative model system for primary microglia cultures or for animal experiments examining brain inflammation. *Altex* **26**(2):83-94.

Hooks SB, Callihan P, Altman MK, Hurst JH, Ali MW and Murph MM (2010) Regulators of G-Protein signaling RGS10 and RGS17 regulate chemoresistance in ovarian cancer cells. *Mol Cancer* **9**:289.

Hunt TW, Fields TA, Casey PJ and Peralta EG (1996) RGS10 is a selective activator of G alpha i GTPase activity. *Nature* **383**(6596):175-177.

Hurst JH and Hooks SB (2009) Regulator of G-protein signaling (RGS) proteins in cancer biology. *Biochem Pharmacol* **78**(10):1289-1297.

Kimura A, Ohmori T, Ohkawa R, Madoiwa S, Mimuro J, Murakami T, Kobayashi E, Hoshino Y, Yatomi Y and Sakata Y (2007) Essential roles of sphingosine 1-phosphate/S1P1 receptor axis in the migration of neural stem cells toward a site of spinal cord injury. *Stem cells* **25**(1):115-124.

Lee JK, Chung J, McAlpine FE and Tansey MG (2011) Regulator of G-protein signaling-10 negatively regulates NF-kappaB in microglia and neuroprotects dopaminergic neurons in hemiparkinsonian rats. *The Journal of neuroscience : the official journal of the Society for Neuroscience* **31**(33):11879-11888.

Lee JK, Kannarkat GT, Chung J, Joon Lee H, Graham KL and Tansey MG (2016) RGS10 deficiency ameliorates the severity of disease in experimental autoimmune encephalomyelitis. *Journal of neuroinflammation* **13**:24.

Lee JK, McCoy MK, Harms AS, Ruhn KA, Gold SJ and Tansey MG (2008) Regulator of G-protein signaling 10 promotes dopaminergic neuron survival via regulation of the microglial inflammatory response. *The Journal of neuroscience : the official journal of the Society for Neuroscience* **28**(34):8517-8528.

Lee JK and Tansey MG (2015) Physiology of RGS10 in Neurons and Immune Cells. *Progress in molecular biology and translational science* **133**:153-167.

Levison SW and McCarthy KD (1991) Characterization and partial purification of AIM: a plasma protein that induces rat cerebral type 2 astroglia from bipotential glial progenitors. *Journal of neurochemistry* **57**(3):782-794.

Lu WH, Wang CY, Chen PS, Wang JW, Chuang DM, Yang CS and Tzeng SF (2013) Valproic acid attenuates microgliosis in injured spinal cord and purinergic P2X4 receptor expression in activated microglia. *Journal of neuroscience research* **91**(5):694-705.

Lv L, Sun Y, Han X, Xu C-c, Tang Y-P and Dong Q (2011) Valproic acid improves outcome after rodent spinal cord injury: potential roles of histone deacetylase inhibition. *Brain research* **1396**:60-68.

Nayak D, Huo Y, Kwang WX, Pushparaj PN, Kumar SD, Ling EA and Dheen ST (2010) Sphingosine kinase 1 regulates the expression of proinflammatory cytokines and nitric oxide in activated microglia. *Neuroscience* **166**(1):132-144.

Nishiguchi KM, Sandberg MA, Kooijman AC, Martemyanov KA, Pott JW, Hagstrom SA, Arshavsky VY, Berson EL and Dryja TP (2004) Defects in RGS9 or its anchor protein R9AP in patients with slow photoreceptor deactivation. *Nature* **427**(6969):75-78.

Noda H, Takeuchi H, Mizuno T and Suzumura A (2013) Fingolimod phosphate promotes the neuroprotective effects of microglia. *Journal of neuroimmunology* **256**(1-2):13-18.

Okahisa Y, Kodama M, Takaki M, Inada T, Uchimura N, Yamada M, Iwata N, Iyo M, Sora I, Ozaki N and Ujike H (2011) Association between the Regulator of G-protein Signaling 9 Gene and

Patients with Methamphetamine Use Disorder and Schizophrenia. *Current neuropharmacology* **9**(1):190-194.

Posner BA, Mukhopadhyay S, Tesmer JJ, Gilman AG and Ross EM (1999) Modulation of the affinity and selectivity of RGS protein interaction with G alpha subunits by a conserved asparagine/serine residue. *Biochemistry* **38**(24):7773-7779.

Raghavendra V, Tanga F and DeLeo JA (2003) Inhibition of microglial activation attenuates the development but not existing hypersensitivity in a rat model of neuropathy. *JPharmacolExpTher* **306**(2):624-630.

Raveh A, Schultz PJ, Aschermann L, Carpenter C, Tamayo-Castillo G, Cao S, Clardy J, Neubig RR, Sherman DH and Sjogren B (2014) Identification of protein kinase C activation as a novel mechanism for RGS2 protein upregulation through phenotypic screening of natural product extracts. *Mol Pharmacol* **86**(4):406-416.

Saito O, Svensson CI, Buczynski MW, Wegner K, Hua XY, Codeluppi S, Schaloske RH, Deems RA, Dennis EA and Yaksh TL (2010) Spinal glial TLR4-mediated nociception and production of prostaglandin E(2) and TNF. *Br J Pharmacol* **160**(7):1754-1764.

Schwartz M, Kipnis J, Rivest S and Prat A (2013) How do immune cells support and shape the brain in health, disease, and aging? *The Journal of neuroscience : the official journal of the Society for Neuroscience* **33**(45):17587-17596.

Seltzer Ze, Dubner R and Shir Y (1990) A novel behavioral model of neuropathic pain disorders produced in rats by partial sciatic nerve injury. *Pain* **43**(2):205-218.

Sjogren B, Parra S, Heath LJ, Atkins KB, Xie ZJ and Neubig RR (2012) Cardiotonic steroids stabilize regulator of G protein signaling 2 protein levels. *Mol Pharmacol* **82**(3):500-509.

Sorge RE, LaCroix-Fralish ML, Tuttle AH, Sotocinal SG, Austin JS, Ritchie J, Chanda ML, Graham AC, Topham L, Beggs S, Salter MW and Mogil JS (2011) Spinal cord Toll-like receptor 4 mediates inflammatory and neuropathic hypersensitivity in male but not female mice. *The Journal of neuroscience : the official journal of the Society for Neuroscience* **31**(43):15450-15454.

Stevens B, Allen NJ, Vazquez LE, Howell GR, Christopherson KS, Nouri N, Micheva KD, Mehalow AK, Huberman AD, Stafford B, Sher A, Litke AM, Lambris JD, Smith SJ, John SW and Barres BA (2007) The classical complement cascade mediates CNS synapse elimination. *Cell* **131**(6):1164-1178.

Suh HS, Choi S, Khattar P, Choi N and Lee SC (2010) Histone deacetylase inhibitors suppress the expression of inflammatory and innate immune response genes in human microglia and astrocytes. *Journal of neuroimmune pharmacology : the official journal of the Society on NeuroImmune Pharmacology* **5**(4):521-532.

Suzumura A, Mezitis SG, Gonatas NK and Silberberg DH (1987) MHC antigen expression on bulk isolated macrophage-microglia from newborn mouse brain: induction of Ia antigen expression by gamma-interferon. *Journal of neuroimmunology* **15**(3):263-278.

Tanga FY, Nutile-McMenemy N and DeLeo JA (2005) The CNS role of Toll-like receptor 4 in innate neuroimmunity and painful neuropathy. *Proc Natl Acad Sci U S A* **102**(16):5856-5861.

Tham CS, Lin FF, Rao TS, Yu N and Webb M (2003) Microglial activation state and lysophospholipid acid receptor expression. *International journal of developmental neuroscience : the official journal of the International Society for Developmental Neuroscience* **21**(8):431-443.

Trang T, Beggs S and Salter MW (2011) Brain-derived neurotrophic factor from microglia: a molecular substrate for neuropathic pain. *Neuron Glia Biol* **7**(1):99-108.

Vellano CP, Lee SE, Dudek SM and Hepler JR (2011) RGS14 at the interface of hippocampal signaling and synaptic plasticity. *Trends Pharmacol Sci* **32**(11):666-674.

Waugh JL, Lou AC, Eisch AJ, Monteggia LM, Muly EC and Gold SJ (2005) Regional, cellular, and subcellular localization of RGS10 in rodent brain. *J Comp Neurol* **481**(3):299-313.

Weng HR, Gao M and Maixner DW (2014) Glycogen synthase kinase 3 beta regulates glial glutamate transporter protein expression in the spinal dorsal horn in rats with neuropathic pain. *Experimental neurology* **252**:18-27.

Wu FX, Bian JJ, Miao XR, Huang SD, Xu XW, Gong DJ, Sun YM, Lu ZJ and Yu WF (2010) Intrathecal siRNA against Toll-like receptor 4 reduces nociception in a rat model of neuropathic pain. *Int J Med Sci* **7**(5):251-259.

Yoon SY, Patel D and Dougherty PM (2012) Minocycline blocks lipopolysaccharide induced hyperalgesia by suppression of microglia but not astrocytes. *Neuroscience* **221**:214-224.

Zachariou V, Georgescu D, Sanchez N, Rahman Z, DiLeone R, Berton O, Neve RL, Sim-Selley LJ, Selley DE, Gold SJ and Nestler EJ (2003) Essential role for RGS9 in opiate action. *Proceedings of the National Academy of Sciences of the United States of America* **100**(23):13656-13661.

Zhuo M, Wu G and Wu LJ (2011) Neuronal and microglial mechanisms of neuropathic pain. *Molecular brain* **4**:31.

Footnotes

This work was supported by grants from the National Multiple Sclerosis Society (SBH) and the National Institutes of Neurological Disorders and Stroke [RO1NS064289] (HRW).

Reprint requests should be sent to Shelley Hooks, shooks@uga.edu, 250 West Green Street, University of Georgia College of Pharmacy, Athens, GA 30602.

Molecular Pharmacology Fast Forward. Published on December 28, 2016 as DOI: 10.1124/mol.116.106963
This article has not been copyedited and formatted. The final version may differ from this version.

Figure Legends

Figure 1: Suppression of RGS10 enhances CXCL2 signaling in microglia. BV-2 cells were treated with either scrambled siRNA as negative control (NC) or RGS10 siRNA for 48 hours. Cells were starved overnight prior to treatment with CXCL12 (100 ng/ml) for 20 minutes. Cells were lysed and western blotting was performed using specific antibodies against phospho-ERK, total ERK, RGS10, GAPDH. Phospho-ERK and intensity was quantified and normalized to total ERK intensity, and statistical comparison was determined using an unpaired t-test of compiled data form three independent experiments, each with duplicate samples (*: p=0.45).

Figure 2: *Rgs10* transcript and RGS protein suppressed in BV-2 mouse microglial cells following LPS treatment in a dose-dependent fashion. (A) BV2 cells were treated with vehicle (serum free media), 10 ng/ml, 100 ng/ml, 1 µg/ml, and 10 µg/ml LPS for 4 hours. Cells were harvested in Trizol and RNA was isolated. *Rgs10* (top panel) and *Tnfα* (bottom panel) transcripts were quantified using SYBR green RT-PCR reagents and normalized to the housekeeping gene actin ($2^{-\Delta\Delta CT}$). **(B)** BV-2 cells were treated with vehicle, 10 ng/ml, 100 ng/ml, 1 µg/ml, and 10 µg/ml LPS for 24 hours and total cell lysates were collected in SDS sample buffer and assessed using western blotting with RGS10 and GAPDH antibodies. **(C)** BV-2 cells were treated with 100 ng/mL LPS for the times indicated and *Rgs10* transcript expression was determined using SYBR green RT-PCR reagents and normalized to the housekeeping gene actin ($2^{-\Delta\Delta CT}$). Data are compiled from three independent experimental repeats each performed in duplicate. Data were analyzed for statistical differences using an analysis of variance (ANOVA) followed by Tukey's test between groups. *: $p < 0.05$, **: $p < 0.01$, and ***: $p < 0.001$ indicate the levels of significance. Similar RT-PCR results were obtained when normalized to GAPDH (data not shown).

Figure 3. Suppression of spinal RGS10 levels in pSNL model of inflammatory neuropathic pain. **(A)** Tissue slices (10 µm) were obtained the L4-L5 region of mouse spinal cord, and expression of

Molecular Pharmacology Fast Forward. Published on December 28, 2016 as DOI: 10.1124/mol.116.106963
This article has not been copyedited and formatted. The final version may differ from this version.

RGS10 (red) and Iba1 (microglial marker, green) were visualized using immunofluorescence as described in methods. Yellow indicates overlap of RGS10 and Iba1 expression. Center panel: 10X. Left inset: 20X . Right inset: 40X **B.** Spinal dorsal horn (L4-L5) tissue from SHAM (n=3) or pSNL (n=3) mice was isolated 3 days after surgery, subjected to SDS-PAGE separation (one animal per lane), and analyzed using western blotting with RGS10 and β-actin antibody. Data shown are average RGS10 levels normalized to β-actin, +/- SEM. Data were normalized by dividing band intensity of RGS10 immunoblot by band intensity of β-actin immunoblot, and analyzed for statistical significance using an unpaired T-test. *: $p < 0.05$.

Figure 4. 5-Aza-2′-deoxycytidine does not affect LPS-induced suppression of *Rgs10* transcription

(A) BV-2 cells were plated in 12 wells plate and allowed to adhere overnight. Cells were treated with vehicle (serum free media) or LPS (10 ng/ml, for 6 hrs) with or without 5-Aza-2′-deoxycytidine (AZA, 10 μM). Cells were harvested in Triazol and RNA was isolated. mRNA transcript levels were measured by quantitative real-time PCR. Transcripts were normalized to the housekeeping gene actin. **(B)** BV-2 cells were plated in 24 wells plate and allowed to adhere overnight. Cells were treated with either vehicle (serum free media) or LPS (10 ng/ml) for 48 hours with or 5-Aza-2′-deoxycytidine (AZA, 10 μM). Cells were harvested and protein levels were assessed by western blot analysis with RGS10 and GAPDH control antibodies. Data are compiled from three independent experimental repeats each performed in duplicate. Data were analyzed for statistical differences using an analysis of variance (ANOVA) followed by Tukey's test between groups. *: $p < 0.05$, **: $p < 0.01$, and ***: $p < 0.001$ indicate the levels of significance.

Figure 5: HDAC inhibitor Trichostatin A (TSA) enhances basal *Rgs10* expression and blocks LPS-stimulated suppression in microglia. (A) BV-2 cells were plated in 12 wells plate and allowed

to adhere overnight. Cells were treated with vehicle, 100, 250, and 500nM TSA for 24 hours. Cells were harvested in Triazol and RNA was isolated. *Rgs10* transcript was quantified using quantitative RT-PCR relative to actin. **(B)** BV-2 cells were treated with vehicle or 10 ng/mL LPS for 6 hours with or without 100 nM TSA, and *Rgs10* transcript was quantified relative to the actin. **(C)** BV-2 cells were treated with vehicle or 1µg/mL LPS for 4 hours with or without 250 nM TSA, and *Rgs10* transcript was quantified relative to the actin. **(D)** Primary microglia were isolated from 2-4 day old mouse pups as described in Methods. Cells were treated with vehicle or LPS (10 ng/mL) for 6 hours with or without TSA (100 nM). *Rgs10* transcript expression was determined using quantitative RT-PCR relative to actin. **(E)** BV-2 cells were plated in 6 wells plate and allowed to adhere overnight. Cells were treated with either vehicle or LPS (10 ng/ml) for 48 hours with or without TSA (100 nM). Cells were harvested and protein levels were assessed by western blot analysis. Blot presented is a representative of three independent experiments. Densitometry values were normalized to GAPDH loading control and then to vehicle-treated condition (right panel). Data in each graph are compiled from three independent experimental repeats each performed in duplicate. Data were analyzed for statistical differences using an analysis of variance (ANOVA) followed by Tukey's test between groups. *: $p < 0.05$, **: $p < 0.01$, and ***: $p < 0.001$ indicate the levels of significance.

Figure 6. LPS effects on TNFα do not mediate RGS10 silencing. (A) BV-2 cells were treated with LPS and/or TSA (as in Fig.4C) and *Tnfα* transcript was quantified using SYBR Green RT-PCR reagents and normalized to actin control. **(B and C)** BV-2 cells were treated with vehicle or LPS (10 ng/ml, for 6 hrs) with or without the TNF-α receptor antagonist, R-7050 (10 µM). *Rgs10* (**B**) and *IL-1β* (**C**) transcript levels were measured by quantitative real-time PCR and normalized to the housekeeping gene actin. R-7050 treatment had no effect on *Rgs10* suppression, but robust effects on IL-1β confirm effective inhibition. **(D)** BV-2 cells were treated with either vehicle or LPS (10 ng/ml) for 48 hours with or without R7050 (10µM). Cells were harvested and protein levels were assessed by western blot analysis with

Molecular Pharmacology Fast Forward. Published on December 28, 2016 as DOI: 10.1124/mol.116.106963
This article has not been copyedited and formatted. The final version may differ from this version.

RGS10 and GAPDH antibodies. Quantitative data in **A-C** are compiled from three independent experimental repeats each performed in duplicate. Data were analyzed for statistical differences using an analysis of variance (ANOVA) followed by Tukey's test between groups. *: $p < 0.05$, **: $p < 0.01$, and ***: $p < 0.001$ indicate the levels of significance. Blot presented in **D** is representative of two independent experiments.

Figure 7. LPS increases HDAC1 binding and decreases histone H3 acetylation at the *Rgs10* promoter in BV2 cells. ChIP assays were carried out in LPS (100 ng/ml) treated and vehicle treated BV-2 cells. Lysates were immunoprecipitated with control, anti-HDAC1 (**A**), anti-acetyl histone H3 (**B**), or anti-histone H3 (**C**) antibodies. Associated DNA was isolated and analyzed via RT-PCR using primers and probes (see Methods) spanning the *Rgs10* promoter and *GAPDH* promoters. Real-time PCR values were normalized to the total amount of DNA added (input). Input values represent 5% of the total cell lysate. Values were normalized to *GAPDH* promoter and represent mean ± SEM of two independent experiments, and RT-PCR reactions were run in triplicate reactions. Data were analyzed using the SDS 2.0 program and significance was tested using a T-test. *: $p < 0.05$.

Figure 8. S1P upregulates *Rgs10* expression and histone acetylation at RGS10 promoters in BV-2. (A) BV-2 cells were serum starved overnight and treated with vehicle or S1P (10 μM) for 48 hours, and then *Rgs10* mRNA was isolated and assessed with RT-PCR relative to actin controls as described. **B**. Acetylated and total H3 Histone ChIP assays were carried out as described in BV-2 cells treated with vehicle or S1P (10 μM). Lysates were immunoprecipitated with control, anti-histone H3, or anti-acetyl histone H3 antibodies. Associated DNA was isolated and analyzed via RT-PCR using primers and probes spanning the *Rgs10* promoter and *GAPDH* promoter. Real-time PCR values obtained were normalized to the total amount of DNA added (input). Input values represent 5% of the total cell lysate.

Molecular Pharmacology Fast Forward. Published on December 28, 2016 as DOI: 10.1124/mol.116.106963
This article has not been copyedited and formatted. The final version may differ from this version.

Rgs10 promoter values were normalized to *GAPDH* promoter values and represent mean ± SEM of two independent experiments, and RT-PCR reactions were run in triplicate reactions. Data were analyzed using the SDS 2.0 program and significance was tested using a T-test. *: $p < 0.05$, **: $p < 0.01$, and ***: $p < 0.001$.

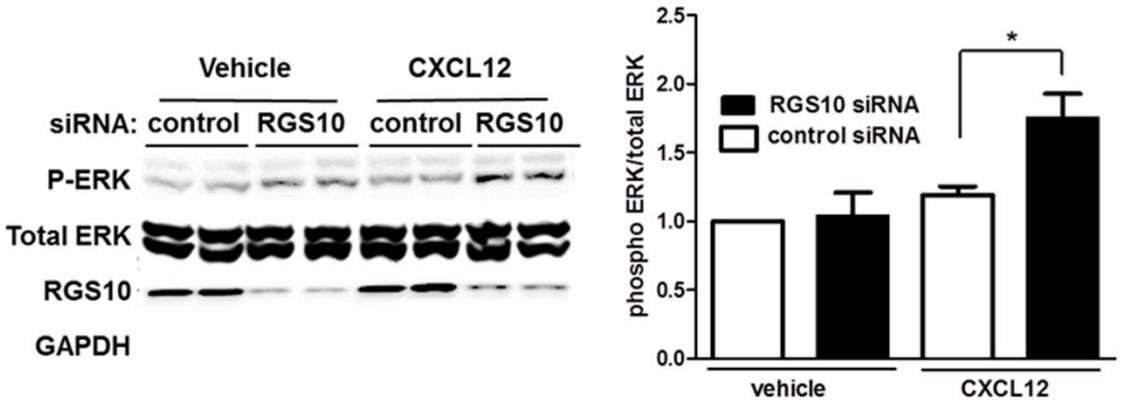

Figure 1

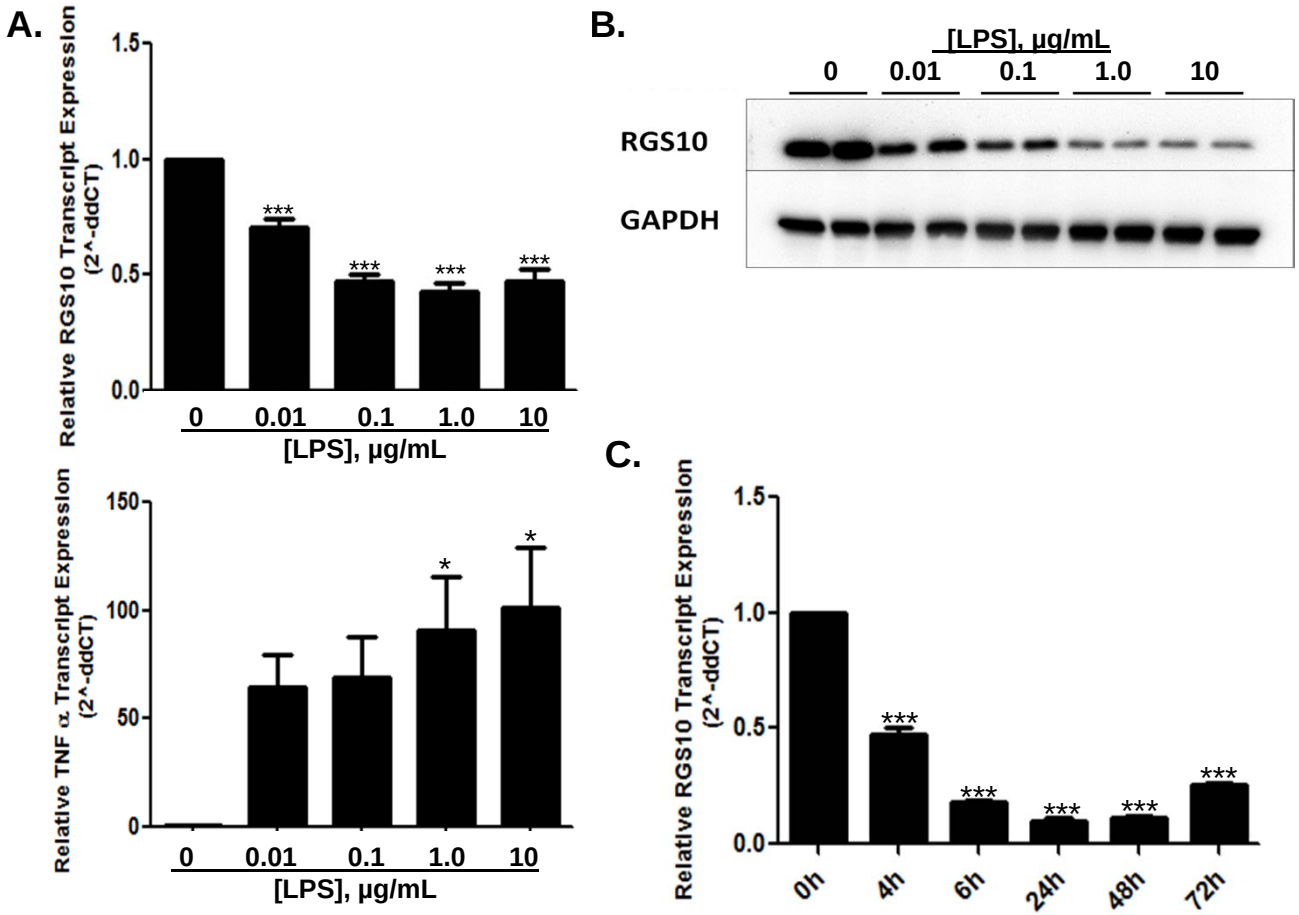

Figure 2

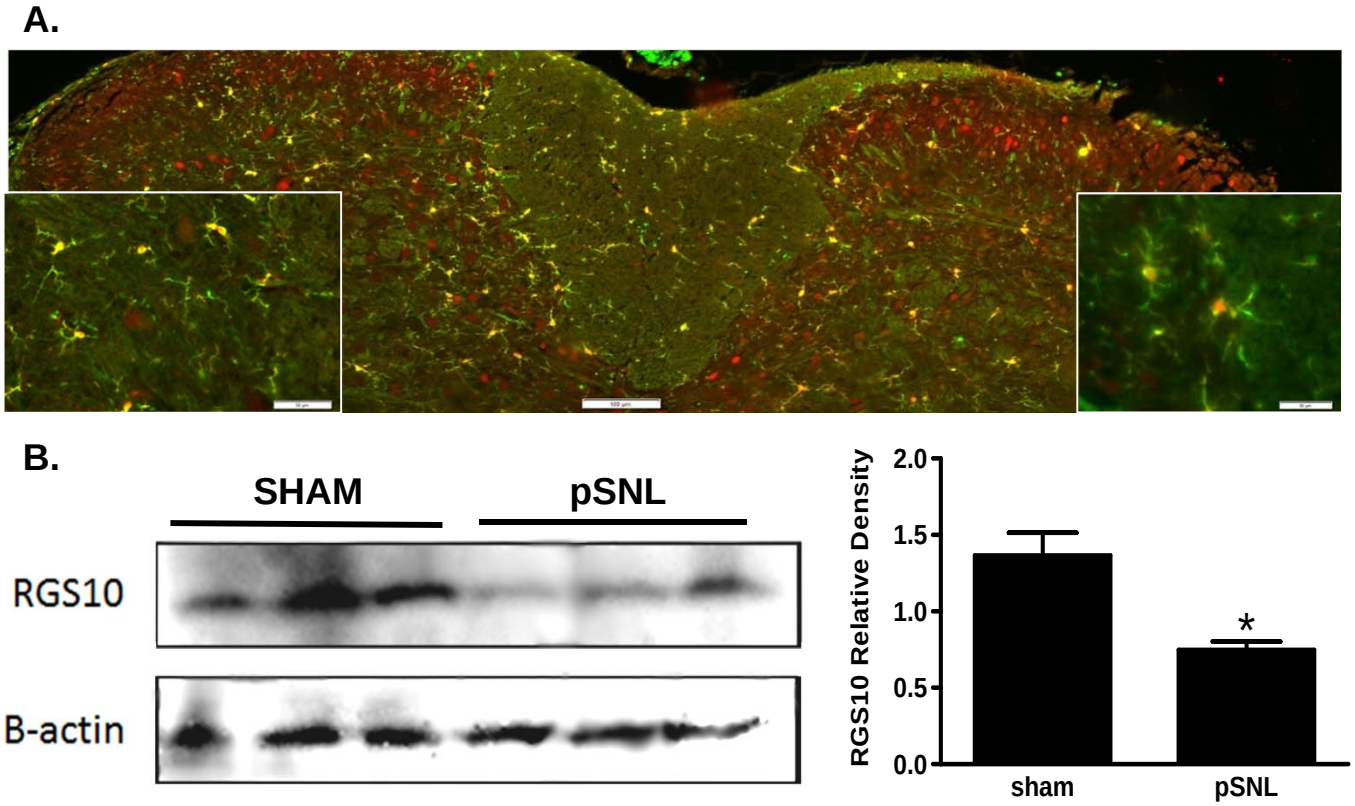

Figure 3

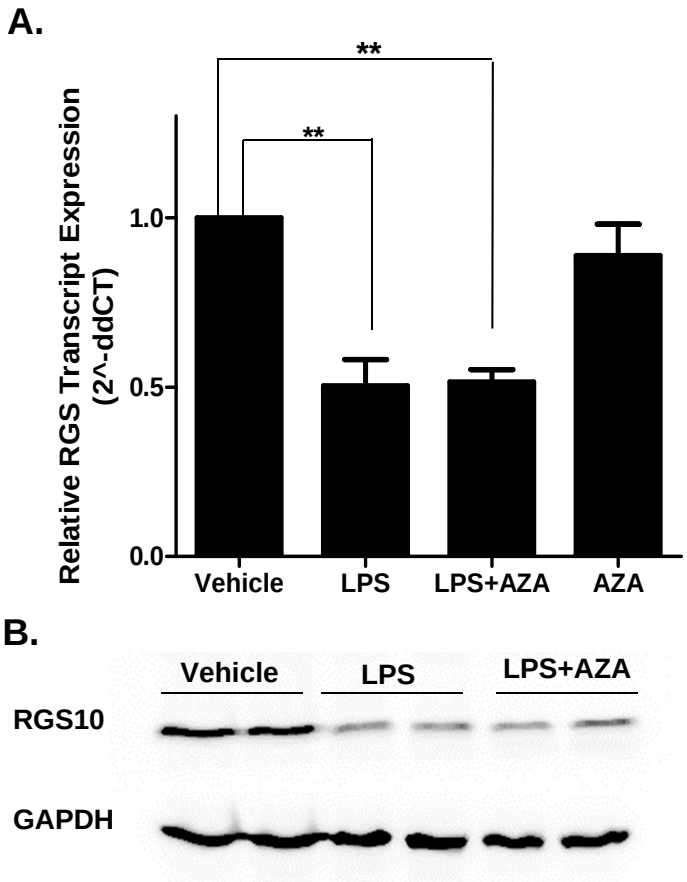

Figure 4

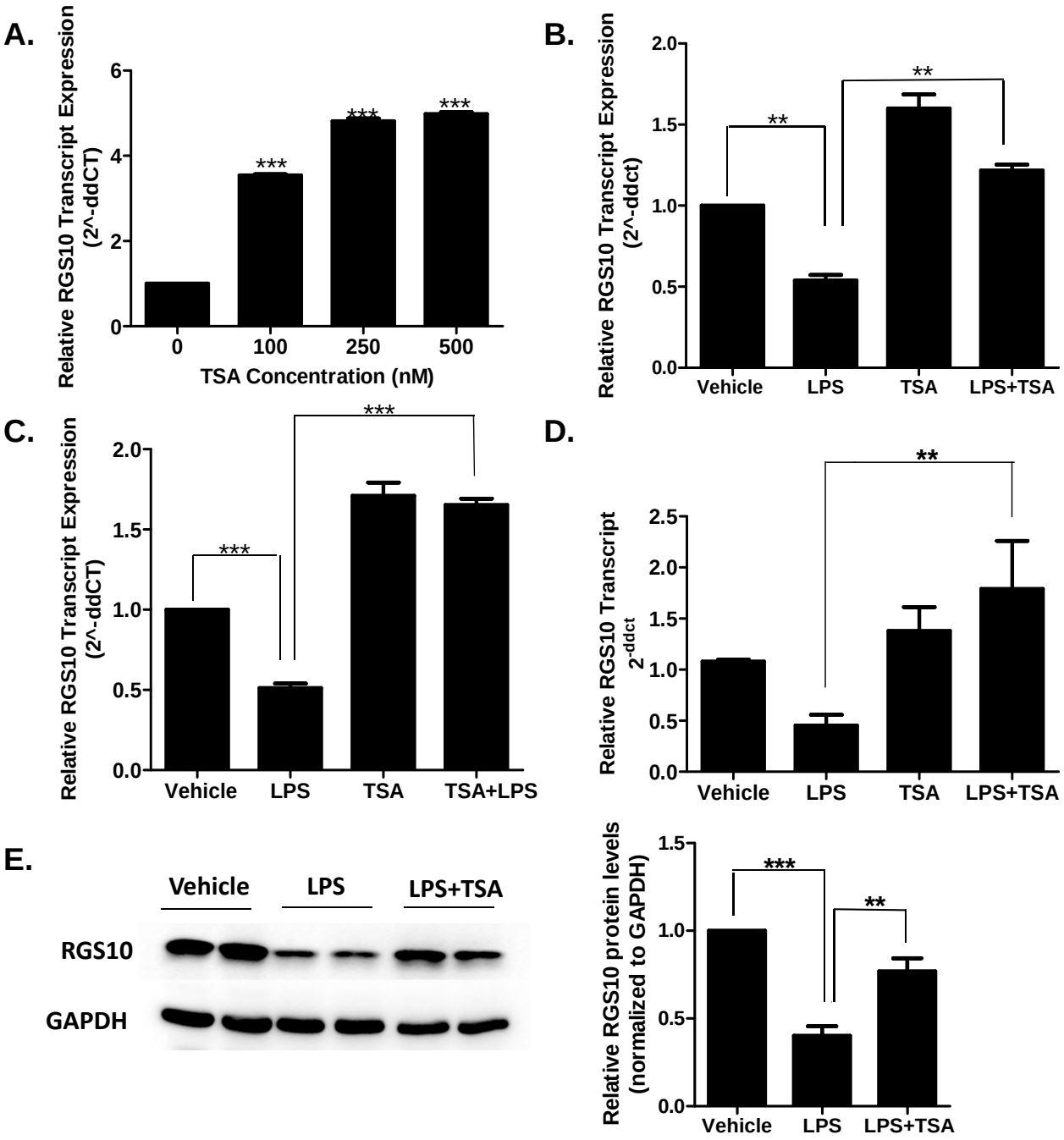

Figure 5

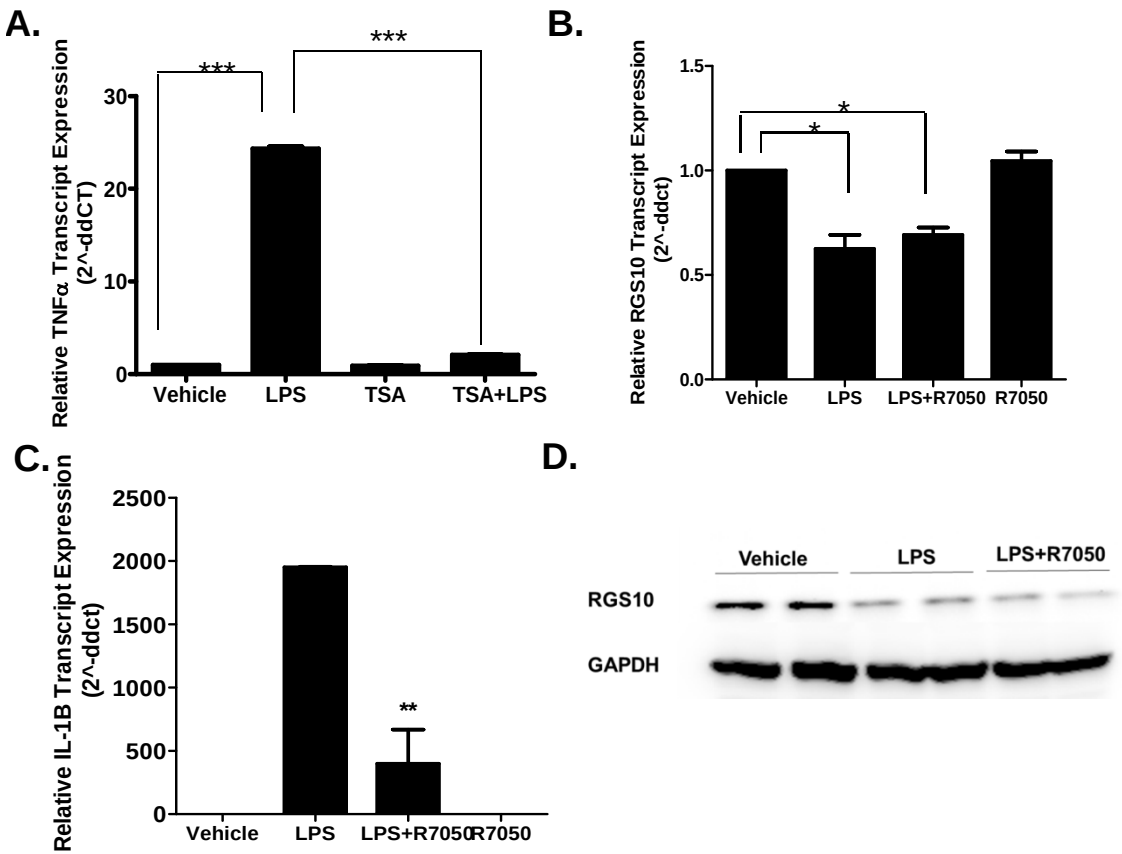

Figure 6

Molecular Pharmacology Fast Forward. Published on December 28, 2016 as DOI: 10.1124/mol.116.106963
This article has not been copyedited and formatted. The final version may differ from this version.

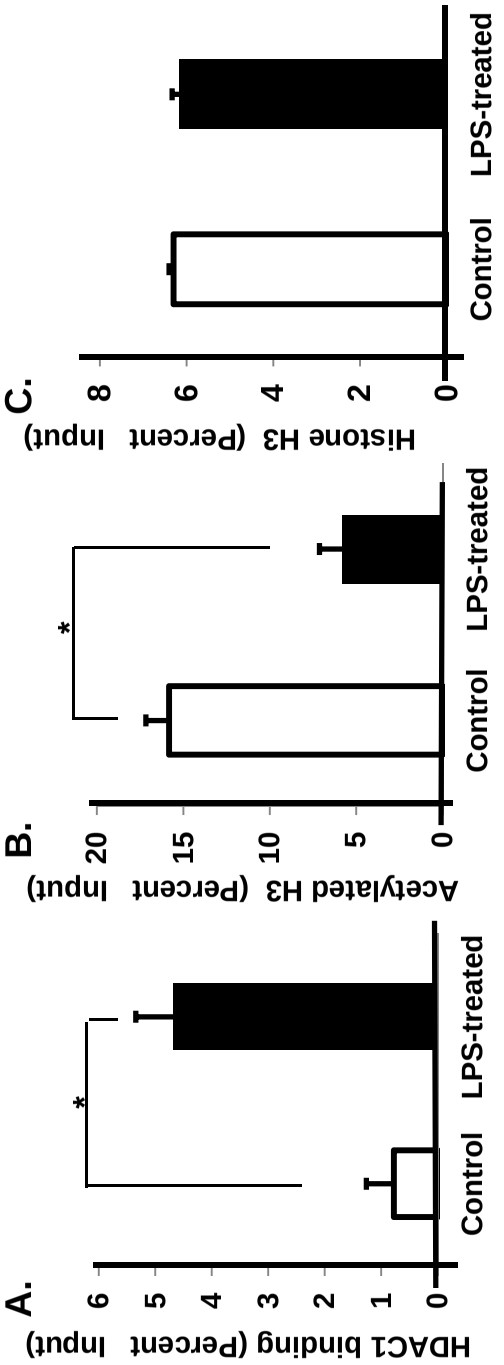

Figure 7

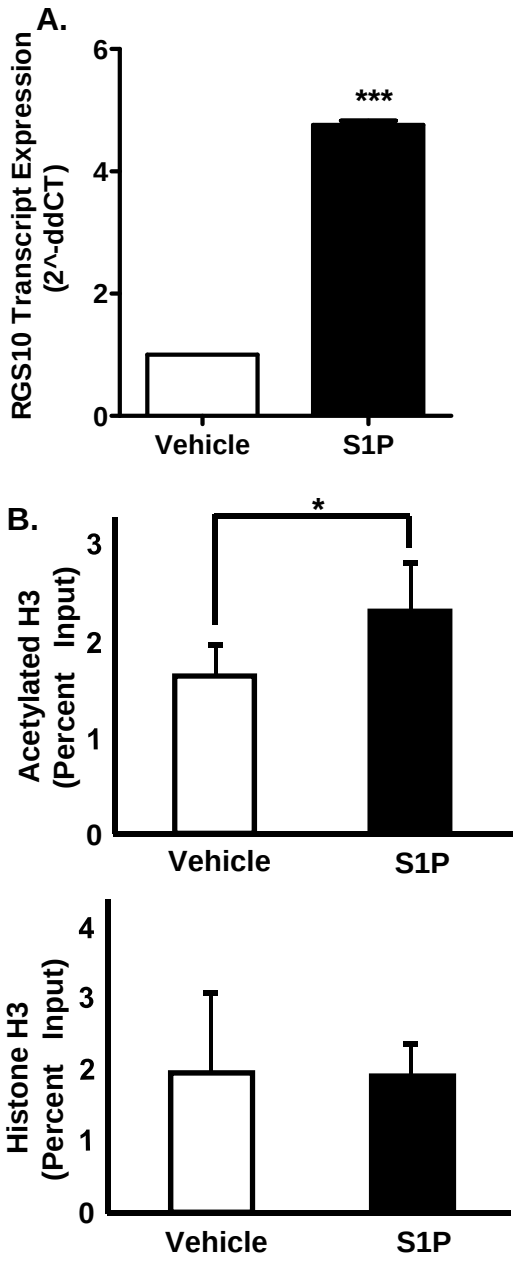

Figure 8